AAS 01-330

A Non-Linear Approach to Spacecraft Formation Control in the Vicinity of a Collinear Libration Point

Richard J. Luquette* and Robert M. Sanner**

Abstract

An expanding interest in mission design strategies that exploit libration point regions demands the continued development of enhanced, efficient, control algorithms for station-keeping and formation maintenance. This paper discusses the development of a non-linear, formation maintenance, control algorithm for trajectories in the vicinity of a libration point. However, the formulation holds for any trajectory governed by the equations of motion for the restricted three body problem. The control law guarantees exponential convergence, based on a Lyaponov analysis. FreeFlyer® and MATLAB® provide the simulation environment for controller performance evaluation. The simulation, modeled after the MAXIM Pathfinder mission, maintains the relative position of a "follower" spacecraft with respect to a "leader" spacecraft, stationed near the L2 libration point in the Sun-Earth system. Evaluation metrics are fuel usage and tracking accuracy.

INTRODUCTION

The restricted-three body problem examines the behavior of an infinitesimal mass in the combined gravitational field of two finite masses rotating in an orbit about their common center of mass. Research on this problem began prior to 1772, the year Lagrange published a set of particular solutions known as the Lagrange or libration points. Libration points, defined within a rotating two body system, represent locations within the rotating frame at which the dynamical forces due to gravity and rotation are neutralized. The equilibrium points are grouped in a set of three collinear points, referred to as L1, L2 and L3; and a set of two triangular points, L4 and L5. With our emerging capability to implement space-based missions, a growing research interest is focused on methods for exploiting the dynamic environment in the vicinity of these points. Some of these missions involve satellite formations. The MAXIM mission and its precursor, MAXIM Pathfinder, fall into this category. Missions of this type carry a requirement for high precision formation control. With this motivation this paper extends the work presented in reference 1, through formulation of a nonlinear control algorithm to achieve this goal.

* Aerospace Engineer. Guidance Navigation and Control Center, NASA-Goddard Space Flight Center, Greenbelt, MD 20771
Tel: (301) 286-5881, Fax: (301) 286-0369, Email: rich.luquette@gsfc.nasa.gov

** Associate Professor, University of Maryland, Aerospace Engineering Department, College Park, MD 20742
Tel: (301) 405-1928, Fax: (301) 314-9001, Email: rmsanner@eng.umd.edu

The control algorithm is based on an Euler-Lagrange (Hamiltonian) formulation of the system dynamics. Ref. 2 details the development of the strategy along with a discussion and proofs of the stability and convergence properties. Ref. 4 applies this formulation to the problem of formation control in the context of the two-body problem. With a different set of dynamics, ref. 1 demonstrates the feasibility of employing this method for trajectory maintenance in the context of the restricted three-body problem. Although this trajectory control strategy is applicable to the problem of formation maintenance, it is deemed impractical due to its dependence on knowledge of the absolute spacecraft position in the rotating reference frame. This paper proposes a preferred strategy, which computes the required control based only on the relative state (position and motion) between the two spacecraft. As before, the control law is exponentially stable, and in the absence of noise, yields zero tracking error.

THEORY

The dynamics (1) and kinematics (2) for most physical systems can be expressed in the Hamiltonian (or Euler-Lagrange) form[1,2].

$$\mathbf{H(q)} * \dot{\mathbf{v}} + \mathbf{C(q,v)} * \mathbf{v} + \mathbf{E(q,v)} = \mathbf{u} \tag{1}$$

$$\dot{\mathbf{q}} = \mathbf{J(q)} * \mathbf{v} \tag{2}$$

Where:

$\mathbf{q}$ – Configuration Variables
$\mathbf{v}$ – Velocity Variables
$\mathbf{H(q)} = \mathbf{H(q)}^T > \mathbf{0}, \forall \mathbf{q}, \mathbf{v}$

$\mathbf{C(q,v)}$ is defined such that $\dot{\mathbf{H}}(\mathbf{q}) - \mathbf{2} * \mathbf{C(q,v)}$ is skew for all $\mathbf{q}, \mathbf{v}$.
For the case that $\dot{\mathbf{q}} = \mathbf{v}$, i.e. $\mathbf{J(q)} = \mathbf{I}$, the dynamic Eq. (1) becomes:

$$\mathbf{H(q)} * \ddot{\mathbf{q}} + \mathbf{C(q,\dot{q})} * \dot{\mathbf{q}} + \mathbf{E(q,\dot{q})} = \mathbf{u} \tag{3}$$

The control law

$$\mathbf{u(t)} = \mathbf{H(q)} * \ddot{\mathbf{q}}_r + \mathbf{C(q,\dot{q})} * \dot{\mathbf{q}}_r + \mathbf{E(q,\dot{q})} - \mathbf{K}_d * \mathbf{s(t)} \tag{4}$$

provides globally stable tracking of a desired trajectory, $\mathbf{q_d}(t)$, such that the tracking error, $\mathbf{e(t)} = \mathbf{q(t)} - \mathbf{q_d(t)}$, exponentially decays to zero.

Note: $\dot{\mathbf{q}}_r(t) = \dot{\mathbf{q}}_d(t) - \Lambda * \mathbf{e(t)}$, $\Lambda = \Lambda^T > 0$, and $\mathbf{s(t)} = \dot{\mathbf{e}}(t) + \Lambda * \mathbf{e(t)} = \dot{\mathbf{q}}(t) - \dot{\mathbf{q}}_r(t)$ (5)

In the presence of dynamic uncertainty with a linear form

$$\mathbf{H(q)} * \ddot{\mathbf{q}} + \mathbf{C(q,\dot{q})} * \dot{\mathbf{q}} + \mathbf{E(q,\dot{q})} = \mathbf{Y(q,\dot{q},q_d,\dot{q}_d)} * \mathbf{a},$$

where $\mathbf{Y(q,\dot{q},q_d,\dot{q}_d)}$ is known. $\mathbf{a}$ is a constant, unknown, vector.

perfect tracking is achieved with the following control law and adaptive rule[2]

$$\mathbf{u} = \mathbf{Y(q,\dot{q},q_r,\dot{q})} * \hat{\mathbf{a}} - \mathbf{K}_d * \mathbf{s},$$
$$\text{with } \dot{\hat{\mathbf{a}}} = -\Gamma * \mathbf{Y(q,\dot{q},q_r,\dot{q})} * \mathbf{s}, \quad \Gamma = \Gamma^T > \mathbf{0} \tag{6}$$

THE RESTRICTED-THREE BODY PROBLEM

The restricted-three body problem considers the dynamics of a small mass (spacecraft) under the gravitational influence of two primary masses (rotating about their common, inertially-fixed, center of mass) . The spacecraft (S/C) dynamics (per unit mass) in inertial coordinates are given by:

$$ {}^{I}\ddot{\mathbf{r}}_{sc} = -GM_1 * {}^{I}\mathbf{r}_{1s}/\|\mathbf{r}_{1s}\|_2^3 - GM_2 * {}^{I}\mathbf{r}_{2s}/\|\mathbf{r}_{2s}\|_2^3 + {}^{I}\mathbf{f}_d \tag{7} $$

where:

GM_i = Gravitational Parameter of Mass i
${}^{I}\mathbf{r}_{is}$ = Position of S/C with respect to Mass i
${}^{I}\mathbf{r}_{sc}$ = Position of S/C
${}^{I}\mathbf{f}_d$ = Unmodeled Disturbance Forces

Alternatively, the dynamics are expressed in a rotating frame defined by the motion of the smaller primary.

$$ {}^{r}\mathbf{u} = \mathbf{A}_{ir}^{T} * {}^{I}\mathbf{u} = \mathbf{H} * {}^{r}\ddot{\mathbf{r}} + \mathbf{C} * {}^{r}\dot{\mathbf{r}} + \mathbf{E}({}^{r}\mathbf{r}) + \mathbf{A}_{ir}^{T} * {}^{I}\mathbf{f}_d \tag{8} $$

where:

${}^{I}\mathbf{r} = \mathbf{A}_{ir} * {}^{r}\mathbf{r}$, ${}^{r}\mathbf{r}$ represents the position vector in the rotating coordinates

$\mathbf{A}_{ir} = [\hat{\mathbf{i}}, \hat{\mathbf{j}}, \hat{\mathbf{k}}]$, $\hat{\mathbf{i}} = {}^{I}\mathbf{r}_2/\|{}^{I}\mathbf{r}_2\|_2, \hat{\mathbf{k}} = ({}^{I}\mathbf{r}_2 \times {}^{I}\mathbf{v}_2)/\|({}^{I}\mathbf{r}_2 \times {}^{I}\mathbf{v}_2)\|_2, \hat{\mathbf{j}} = \hat{\mathbf{k}} \times \hat{\mathbf{i}}$

${}^{I}\mathbf{r}_2, {}^{I}\mathbf{v}_2$ represent the inertial position and velocity of the smaller primary relative to the center of the rotating frame.

$\mathbf{H} = \mathbf{I}_3$

$\mathbf{C} = 2 * \mathbf{A}_{ir}^{T} * \dot{\mathbf{A}}_{ir} = 2 * \mathbf{A}_{ir}^{T} * \mathbf{A}_{ir} * \boldsymbol{\Omega} = 2 * \boldsymbol{\Omega}$

$\mathbf{E}({}^{r}\mathbf{r}) = \mathbf{A}_{ir}^{T} * (\ddot{\mathbf{A}}_{ir} * {}^{r}\mathbf{r} + GM_1 * {}^{I}\mathbf{r}_{1s}/\|\mathbf{r}_{1s}\|_2^3 + GM_2 * {}^{I}\mathbf{r}_{2s}/\|\mathbf{r}_{2s}\|_2^3)$

$\boldsymbol{\Omega} = \mathbf{Skew}\{({}^{r}\mathbf{r} \times {}^{r}\mathbf{v})/\|\mathbf{r}\|_2\}$

Note: $[\dot{\mathbf{H}}(t) - 2 * \mathbf{C}(\mathbf{q}, \dot{\mathbf{q}})] = 2 * \boldsymbol{\Omega}$, which is skew symmetric.

It is important to note that the motion of the two primary masses define $\mathbf{A}_{ir}$, and it's derivatives. Hence, the behavior of $\mathbf{A}_{ir}$ is generally well known and predictable for trajectories within our solar system.

DYNAMICS OF RELATIVE MOTION

With dynamics defined by Eqs. 7 or 8, implementation of an adaptive control strategy, Eq. (6), provides perfect tracking of a predefined trajectory for station-keeping within the assumed constraints[1]. The method equally applies to the problem of formation maintenance, but requires knowledge of the spacecraft's position within the rotating frame. Practical considerations preference a strategy based on the relative motion between two spacecraft. For the simple case of a leader/follower formation, Eq. (7) yields the relative dynamics between the two spacecraft

$$ {}^{I}\ddot{\mathbf{x}} = -GM_1 * ({}^{I}\mathbf{r}_{1F}/\|\mathbf{r}_{1F}\|_2^3 - {}^{I}\mathbf{r}_{1L}/\|\mathbf{r}_{1L}\|_2^3) - GM_2 * ({}^{I}\mathbf{r}_{2F}/\|\mathbf{r}_{2F}\|_2^3 - {}^{I}\mathbf{r}_{2L}/\|\mathbf{r}_{2L}\|_2^3) + {}^{I}\mathbf{f}_d + (\mathbf{u}_F - \mathbf{u}_L) \tag{9} $$

where the subscript 'L' refers to the leader spacecraft, 'F' to the follower spacecraft, and ${}^{I}\mathbf{x} = {}^{I}\mathbf{r}_F - {}^{I}\mathbf{r}_L$. The disturbance force, symbolically unchanged, now represents the disturbance effect on the relative motion of the two spacecraft. In rotational coordinates the dynamics assume a form similar to Eq. (8).

However, the transformation is unnecessary, since both the measurements and the desired relative trajectory are readily resolved in inertial space.

Manipulating the terms in Eq. (9) results in the equivalent expression

$$ {}^{I}\ddot{\mathbf{x}} = -(GM_1/\|\mathbf{r}_{1F}\|_2^3 + GM_2/\|\mathbf{r}_{2F}\|_2^3) * {}^{I}\mathbf{x} - GM_1 * {}^{I}\mathbf{r}_{1L} * (\|\mathbf{r}_{1F}\|_2^{-3} - \|\mathbf{r}_{1L}\|_2^{-3}) - GM_2 * {}^{I}\mathbf{r}_{2L} (\|\mathbf{r}_{2F}\|_2^{-3} - \|\mathbf{r}_{2L}\|_2^{-3}) + {}^{I}\mathbf{f}_d + (\mathbf{u}_F - \mathbf{u}_L) \quad (10) $$

The first term denotes a differential acceleration, oriented along the spacecraft separation vector. The second and third terms represent differential accelerations along the separation vectors between the primaries and the leader spacecraft. For a formation requirement with a constant $\mathbf{x}$, the first term will remain inertially fixed, possibly varying in magnitude. For slow moving trajectories in the rotating frame of the three-body problem, this magnitude is considered constant over short time intervals. Additionally, the second and third terms are considered fixed in the rotating coordinate frame. This observation suggests the gravitational influence of the primaries are represented as:

$ {}^{I}\mathbf{f}_d = \Gamma * \mathbf{a} $, where $ \Gamma = [\mathbf{A}_{Ir} \vdots \mathbf{I}_3] $, and $\mathbf{a}$ is slowly varying, possibly constant.

CONTROL LAW DESIGN

The combined results of the two preceding sections generate the control law.

$$ \begin{aligned} &\mathbf{u}_F = {}^{I}\ddot{\mathbf{x}}_r + GM_1 * ({}^{I}\mathbf{r}_{1F}/\|\mathbf{r}_{1F}\|_2^3 - {}^{I}\mathbf{r}_{1L}/\|\mathbf{r}_{1L}\|_2^3) + GM_2 * ({}^{I}\mathbf{r}_{2F}/\|\mathbf{r}_{2F}\|_2^3 - {}^{I}\mathbf{r}_{2L}/\|\mathbf{r}_{2L}\|_2^3) + {}^{I}\mathbf{f}_d + \mathbf{u}_L - \mathbf{K}_d * \mathbf{s} \\ &\text{with } \dot{\mathbf{x}}_r = \dot{\mathbf{x}}_d - \Lambda * (\mathbf{x} - \mathbf{x}_d), \quad \mathbf{s} = (\dot{\mathbf{x}} - \dot{\mathbf{x}}_d) + \Lambda * (\mathbf{x} - \mathbf{x}_d) \end{aligned} \quad (11) $$

Here ${}^{I}\mathbf{f}_d$ is an unknown force. Therefore, implementation requires an adaptive strategy to estimate the disturbance contribution. Based on the discussion in the previous section, with a "slow" moving trajectory the gravitational influence of the primaries assumes a linear form. This suggests modeling the disturbance in a similar fashion, allowing an adaptive estimate of ${}^{I}\mathbf{f}_d$ in the control algorithm.

$$ \begin{aligned} &\mathbf{u}_F = \mathbf{u}_L + {}^{I}\ddot{\mathbf{x}}_r + GM_1 * ({}^{I}\mathbf{r}_{1F}/\|\mathbf{r}_{1F}\|_2^3 - {}^{I}\mathbf{r}_{1L}/\|\mathbf{r}_{1L}\|_2^3) + GM_2 * ({}^{I}\mathbf{r}_{2F}/\|\mathbf{r}_{2F}\|_2^3 - {}^{I}\mathbf{r}_{2L}/\|\mathbf{r}_{2L}\|_2^3) + {}^{I}\hat{\mathbf{f}}_d - \mathbf{K}_d * \mathbf{s} \\ &\text{with } {}^{I}\hat{\mathbf{f}}_d = \Gamma * \hat{\mathbf{a}}, \ \dot{\hat{\mathbf{a}}} = -\alpha * \Gamma^T * \mathbf{s}, \text{ where, } \alpha > 0, \Gamma = [\mathbf{A}_{Ir} \vdots \mathbf{I}_3] \end{aligned} \quad (12) $$

Note: computation of the desired control requires knowledge of the position of the two spacecraft referenced to the primary masses. In practice these vectors are estimated, based on various measurements. The estimation error appears as an unmodeled disturbance, which will not conform to the structure of ${}^{I}\mathbf{f}_d$, defined in Eq. (12). However, the gravitational influence of the primaries has the same linear form as the adaptive rule by design. Therefore, the suggested approach estimates the contribution of all gravitational influences and other disturbances.

$$ \begin{aligned} &\mathbf{u}_F = \mathbf{u}_L + {}^{I}\ddot{\mathbf{x}}_r + \Gamma * \hat{\mathbf{a}} - \mathbf{K}_d * \mathbf{s} \\ &\text{with } \dot{\hat{\mathbf{a}}} = -\alpha * \Gamma^T * \mathbf{s}, \text{ where, } \alpha > 0, \Gamma = [\mathbf{A}_{Ir} \vdots \mathbf{I}_3] \end{aligned} \quad (13) $$

Implementation of Eq. (13) requires only local measurement of the relative position and motion between the two spacecraft. As a practical difficulty, the follower spacecraft is required to mirror any control effort imparted to the lead spacecraft. Careful mission planning avoids this situation by limiting the leader spacecraft to infrequent, station-keeping maneuvers, so $\mathbf{u}_L=0$ during precision formation maneuvers. Interchangeability of the leader and follower roles facilitates flexibility in fuel management and station-keeping strategies. Finally, since the gravitational influence from the primaries dominate the disturbance,

the gravity terms in Eq. (12) can be computed to establish a bound on the estimated disturbance, ${}^{I}\hat{\mathbf{f}}_d = \Gamma * \hat{\mathbf{a}}$, in Eq. (13), thus limiting the potential for parameter drift.

SIMULATION

Implementation of the proposed adaptive control law, Eq. (13), is simulated using FreeFlyer® interfaced with MATLAB®. FreeFlyer® supplies the dynamics model and propagation tool. MATLAB® provides the computational tools to determine the control effort at each time step. Additionally, MATLAB® serves to capture and analyze the simulation data.

The design of the simulation scenario is based on the MAXIM Pathfinder mission[3], shown in Figure 1. The mission consists of a two spacecraft formation, designed to demonstrate the feasibility of space-based X-ray interferometry for astronomical applications. Proposals for a nominal mission trajectory include both an orbit about L2 in the Earth-Sun system, and an Earth trailing, drift away orbit. The simulations model both options.

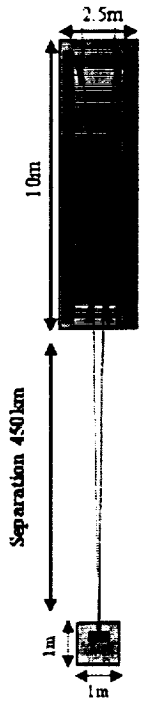

Optics Spacecraft

Carries:	X-ray Interferometers
	Finder X-ray Telescopes
	2 Visible Light Interferometers
	Laser Ranging System
Size:	2.5x2.5x10m
Pitch&Yaw Stability:	$3x10^{-4}$ arcsec
Pitch&Yaw Knowledge:	$3x10^{-5}$ arcsec
Roll Stability:	20 arcsec
Position Stability:	---

Detector Spacecraft

Carries:	X-ray Detector Array
	Laser Retro Reflectors
	Precision Thrusters
Size:	1x1x1m
Pitch&Yaw Stability:	20 arcsec
Roll Stability:	20 arcsec
Lateral Stability:	5mm
Lateral Knowledge:	50 microns
Focal Stability:	10 meters

Figure 1. MAXIM Pathfinder Design

Perturbations include the gravitational influence of the Sun and all the planets, and solar pressure. The Earth's gravitational field model includes zonal and tesseral terms up to J21. The simulation period is 10 days, starting on May 1, 2001. The integration step size is 30 seconds. Each case employs the same gains: $K_d = .05$, $\Lambda = .01$, and $\alpha = 10^{-4}$. The gains, selected by trial and error, are not optimize for system performance. Thrusters are assumed to have full throttling and pointing capability.

The simulation for each case is divided into three phases. In phase I the spacecraft are mechanically linked with the transfer into the final mission trajectory completed. The mechanical link is modeled by initializing both spacecraft with the same position/velocity and commanding a zero separation distance. Phase II models the transition from initial mechanical separation to a nominal formation configuration. Separation is accomplished with a constant continuous thrust applied to the Follower spacecraft. During the first half of the maneuver, the Follower accelerates away from the Leader spacecraft. At the halfway point the thrust is reversed, decelerating the Follower, to reach the mission formation configuration with zero relative velocity to the Leader spacecraft. During Phase III the Follower is commanded to maintain a constant, 450 kilometer, separation with the Leader spacecraft. The Leader spacecraft drifts under the influence of environmental forces with no applied external thrust. For the cases presented the separation is maintained along the inertial x-axis. Simulations with other orientations of the separation vector produced similar results.

Case 1

The spacecraft are stationed in a Lissajous orbit about the L2 point of the Earth-Sun system. The initial state vector was obtained from a simulation for the Mircowave Anisotrophy Probe (MAP) mission. The relative position between the two spacecraft is shown in Figure 2. Phase II starts 6 hours into the

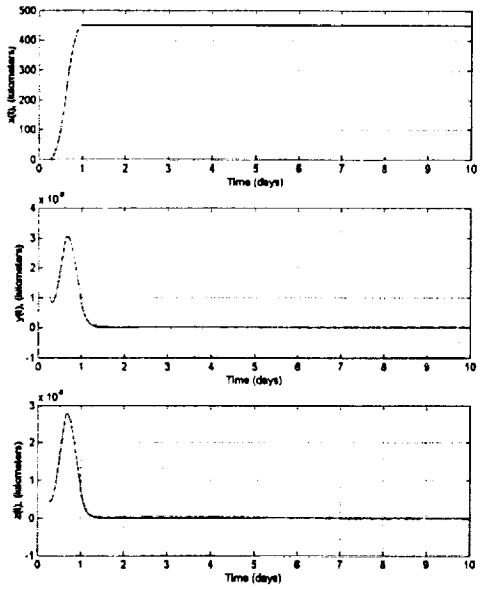

Figure 2. Case 1- Relative Position of Follower Spacecraft to Leader in Inertial Coordinates

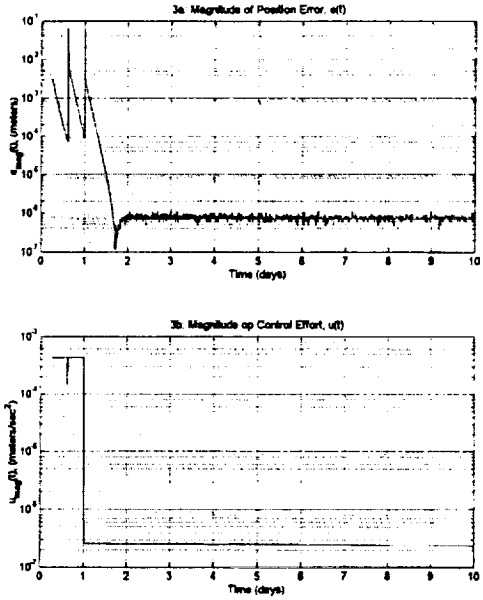

Figure 3. Case 1 – Error Magnitude and Control Effort

simulation, and concludes at the end of day 1. Figure 3 provides the magnitude of the position error and the control thrust. The tracking error is effectively zero, 10^{-7} meters, which reflects the limit of the simulator's machine precision.

As seen in Figure 4, the adaptation law converges to a nearly constant estimate of the vector, $\hat{\mathbf{a}}$. Recall, this vector is expected to vary slowly with time. Transients during the separation maneuver are expected, since the differential gravitational force on the spacecraft will increase with the separation distance. Although the tracking error performance degrades during separation, it remains within a centimeter of the desired trajectory.

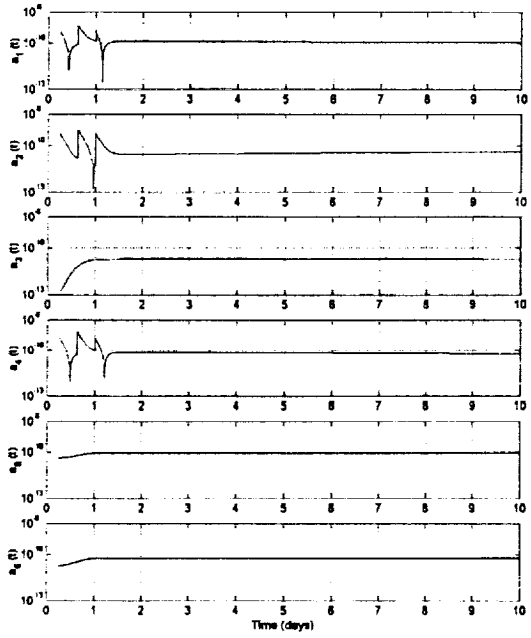

Figure 4. Case 1 – Time History of Adaptation Vector, $\hat{\mathbf{a}}$, (km/sec^2)

Case 2

For this case the spacecraft initial state vectors are set to the values of the Earth's position and velocity 5 days prior to the simulation start time, based on planetary ephemeris data. Thus, the spacecraft trajectory lags the motion of the Earth by

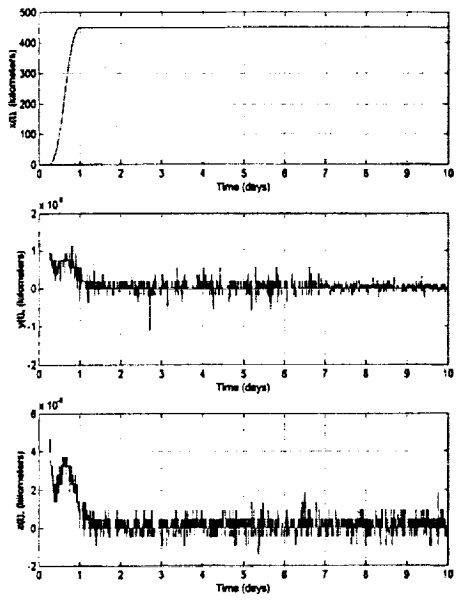

Figure 5. Case 2- Relative Position of Follower Spacecraft to Leader in Inertial Coordinates

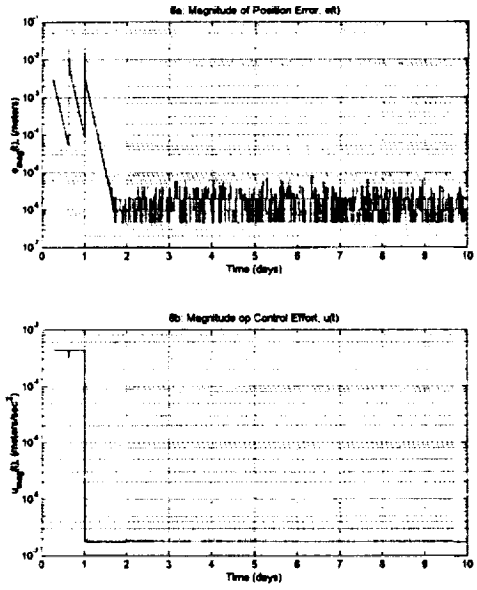

Figure 6. Case 2 – Error Magnitude and Control Effort

approximately 5 degrees. A slight reduction in the velocity was required to cause a "drift away" motion. Simulation results are shown in Figures 5, 6 and 7. As in Case 1, the control law generates perfect tracking within the limit of machine precision. Compared to case 1, it appears less control effort is required to maintain the formation, (1.9e-7 versus 2.5e-7 meters/sec^2). Hence, fuel economy favors Case 2. As with Case 1, the adaptation vector, $\hat{\mathbf{a}}$, assumes a fairly constant value with a slow variation after the separation transient. Further analysis is required to verify this result, since the simulation is operating at the limit of machine precision.

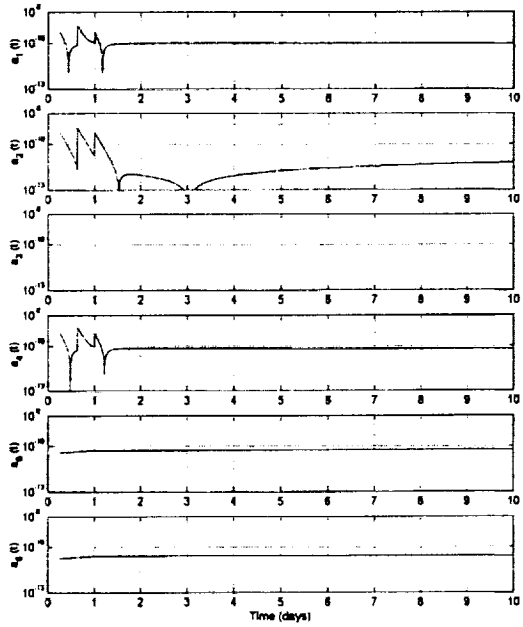

Figure 7. Case 2 – Time History of Adaptation Vector, $\hat{\mathbf{a}}$, (km/sec^2)

Cases without Adaptation

To assess the effectiveness of adaptation the above cases were run with $\hat{\mathbf{a}} = \mathbf{0}$. This reduces the control algorithm to a simple linear PD controller for the Phase III sequence with $\ddot{\mathbf{x}}_d = \mathbf{0}$. The results are displayed in Figures 8 and 9. In both cases the control effort remains essentially unchanged by the lack of adaptation. This is expected. However, the tracking performance degrades, maintaining millimeter accuracy. With a further loss of

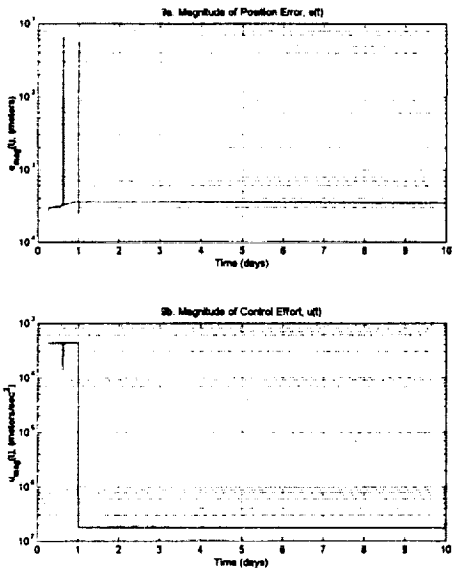

Figure 8. Case 1 without Adaptation – Error Magnitude and Control Effort

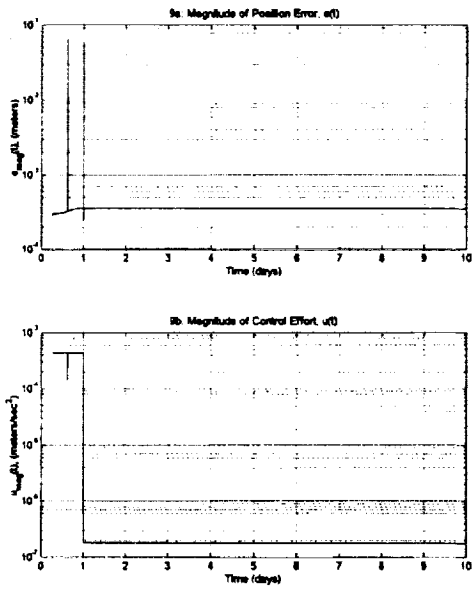

Figure 9. Case 2 without Adaptation – Error Magnitude and Control Effort

performance expected from noise and other disturbances, the adaptive approach is required to satisfy mission requirements.

Conclusion

Adaptive nonlinear control is an effective strategy for maintaining a spacecraft formation with zero tracking error. Implementation of the control only requires measurement of the relative position and velocity of the two spacecraft, reducing the potential sources of measurement errors. The adaptation mechanism effectively compensates for all environmental forces modeled in the simulation.

The simulation does not consider noise sources, such as those associated with measurement error or actuator performance. Further, this strategy is limited to position and velocity control. Missions, such as MAXIM Pathfinder, require simultaneous control of relative position and attitude. Typically, for the case of a single spacecraft translation and attitude maneuvers are coordinated, although control system designs treat the dynamics as uncoupled. For the MAXIM Pathfinder, and similar missions, the dynamics are coupled under assumed constant thrust, requiring a coupled, six-degree of freedom (6DOF) control strategy.

The following items are considered for future work:

- Include robust features to ensure desired performance under various disturbances.
- Design nonlinear, 6DOF Control for spacecraft position and attitude to ensure pointing and position requirements are simultaneously achieved.
- Process measurements with a nonlinear observer, and demonstrate stability of the coupled observer/controller.
- Employ "Realistic" simulation models for testing algorithms. Include modeling of measurement error sources, actuator performance, and other effects.

References:

1. Luquette, R. J. and Sanner, R.M. "A Non-Linear Approach to Spacecraft Trajectory Control in the Vicinity of a Libration Point", Flight Mechanics Symposium, Goddard Space Flight Center June 19-21, 2001.

2. Slotine, J.E. and Li, W., "Applied Nonlinear Control", Prentice Hall, Inc., New Jersey, 1991

3. http://maxim.gsfc.nasa.gov, Micro-Arcsecond X-Ray Interferometry Mission website, Goddard Space Flight Center, May 2001.

4. de Queiroz, M.S., Kapila, V., and Yan, Q., "Adaptive Nonlinear Control of Multiple Spacecraft Formation Flying", Journal of Guidance, Navigation, and Control, Vol. 23, No. 3, May-June 2000.